Investigation of a Two-stage Boost Converter using the Neutral Point of a Motor

Jun-ichi Itoh*, Daisuke Ikarashi*

* Nagaoka University of Technology, 1603-1 Kamitomioka-cho Nagaoka City Niigata 940-2188, Japan

Abstract--**This paper discusses about a six-step operation strategy for a proposed two-stage boost converter using the neutral point of a motor. The proposed converter consists of a small boost chopper and a three-phase inverter, which has a boost up function from the use of the leakage inductance of a motor instead of a boost-up reactor, for a DC to AC conversion. When the inverter part outputs a square waveform of 180 degree, the input current has distortion because the neutral point voltage of the motor is fluctuated at three times of the output frequency. The input current distortion because of the voltage fluctuation is reduced to 1/8 smaller by applying a feed forward control. Additionally, in this proposed circuit, the DC current is imposed into the phase current of the motor. Therefore, the influence of the imposed DC current is investigated in a FEM by simulating a 1.5-kW IPM motor.**

Index Terms--**Boost converter, Feed forward control, Leakage inductance, Six-step operation**

I. INTRODUCTION

Recently, motor drive technologies that drive with a battery are required in a lot of applications such as electric vehicles and rail trains [1]. In order to obtain high efficiency, high terminal voltage at the motor is required. However, a higher voltage will need to increase the volume of the battery bank and result the cost will increase. Therefore, the battery is usually connected to a boost converter before an inverter stage.

Fig. 1 shows the conventional DC/AC power converter, which is composed of batteries, a boost converter and a three-phase inverter. Battery voltage is increased by the boost converter when the inverter outputs high voltage to the motor. However, the boost converter requires a large boost-up reactor which is high cost and bulky. In addition, higher switching frequency is applied in order to reduce the size volume of the boost-up reactor, however this strategy increases the switching losses. As one of solution to reduce the switching losses under high frequency, resonance converters are used [2-4]; however the number of components is increased in the boost-up converter.

The authors have been proposed a reactor free boost-up converter that uses the leakage inductance of a motor instead of a boost-up reactor [5-6]. The proposed converters can increase the inverter output voltage without increasing the number of components. However, when the proposed converter is applied to the DC to AC conversion, the proposed converter is found with the following three problems;

(i) *The limitation of the inverter output voltage*
When the battery is connected to the neutral point of motor, the maximum phase voltage of the inverter is limited by the battery voltage.

(ii) *Ripple current caused by the Six-step operation*
One of the control methods for motor drive is the six-step operation. The six-step operation of the inverter can increase the voltage utilization and achieve higher efficiency than a PWM operation since the switching frequency of a six-step operation is lower than the PWM operation. In the reactor free boost-up converter, when the six-step operation is applied to the inverter control, the neutral point voltage of the motor will fluctuate at a frequency which is three times of the output frequency. Since the battery is connected to the neutral point of the motor, the input current will contain large ripple due to the fluctuation of the neutral point voltage of the motor.

(iii) *Increasing of the motor loss*
In the reactor free boost-up converter, the DC current is imposed into the phase current of the motor. As a result, the copper loss of the motor is increased. Meanwhile, in an ideal condition, the zero-phase current in the motor does not generate motor torque and iron loss because the zero-phase flux is denied with each other. However, the magnetic flux density might be increased by the zero-phase current. Influence of the zero-phase current in the motor has never clarified before.

This paper proposes a two-stage boost converter using the neutral point of a motor to solve the problems (i) and (ii). The proposed circuit consists of batteries, a three-phase inverter which connects to the neutral point of a motor and a small boost-up converter. The proposed circuit can reduce the terminal voltage of a boost-up reactor. As a result, the proposed circuit can reduce the size of the boost-up reactor and switching losses in the boost converter. In addition, the current fluctuation at the neutral point of the motor that resulted from the six-step operation will be compensated by a current regulator and a feed forward control in a small stage boost converter. The validity of the proposed converter and its control strategy are confirmed with a simulation and the experimental results. Furthermore, in consider for the iron loss and the torque ripple, the influence of (iii) is analyzed in a 2D Finite Element Method (FEM) by simulating a 1.5-kW IPM motor.

II. CIRCUIT TOPOLOGY

A. Circuit configuration

Fig. 2 shows the proposed circuit configuration. The proposed circuit is composed of batteries, a three-phase inverter and a first stage boost converter that connects to

the neutral point of a motor. The inverter in the proposed circuit comes with a boost-up function when the motor leakage inductance is utilized. However, the DC current is imposed to the phase current of the motor in the proposed circuit.

The proposed circuit can reduce the volume of the boost-up reactor and switching losses in the first stage boost converter. When a sinusoidal wave triangle carrier comparison method is used to generate PWM pulses, the neutral point voltage of the motor is the same as the neutral point voltage of the DC link part, i.e. half of the DC link voltage E_{dc1}. Therefore, the voltage rating of the boost-up reactor and switching device in the first stage boost converter is reduced to half of the DC link voltage. It should be noted that the capacitor C_2 that is connected to the neutral point of the motor is 100 times smaller than the DC link capacitor C_1 of the inverter.

B. Positive phase sequence equivalent circuit

Fig. 3 shows the positive-phase sequence equivalent circuit of the proposed circuit. The proposed circuit can be divided into a positive and a zero sequence components. The boost converter does not appear in the positive-phase sequence equivalent circuit due to the connection of the neutral point of the motor. Consequently the positive-phase sequence equivalent circuit is similar to a conventional three-phase inverter. During the PWM control, when a sinusoidal modulation based on the triangle carrier comparison is used to generate PWM pulses, the fundamental voltage of the output is given by

$$V_{out} = \frac{\sqrt{3}}{2\sqrt{2}} E_{dc} \cdot a \quad ....(1),$$

where V_{out} is the output line voltage, E_{dc} is the DC link voltage and a is the modulation index.

In the proposed circuit, a six-step operation is applied to the three-phase inverter in order to reduce the switching loss of the inverter in comparison to a PWM inverter. During the six-step operation, the switching frequency agrees with the output frequency. The output line voltage becomes a 120 degree square waveform, then, the fundamental voltage of the output is given by

$$V_{out} = \frac{\sqrt{6}}{\pi} E_{dc} \quad ....(2).$$

C. Zero phase sequence equivalent circuit

Fig. 4 shows the zero-phase sequence equivalent circuit. The back electromotive force (EMF) does not appear in the zero-phase sequence equivalent circuit but only the leakage inductance exists. In zero-phase sequence, the inverter legs could consider as a single leg. Then the output voltage of the single leg is the same as the neutral point voltage of the motor. A two-stage boost up operation is achieved by two choppers, which are constructed by switch S_1, S_2 and switch S_3 and S_4. However, the leakage inductance of the motor decreases to 1/3 since the leakage inductance of the motor is connected in parallel in the zero-phase sequence equivalent circuit.

On the other hand, the neutral point voltage of the
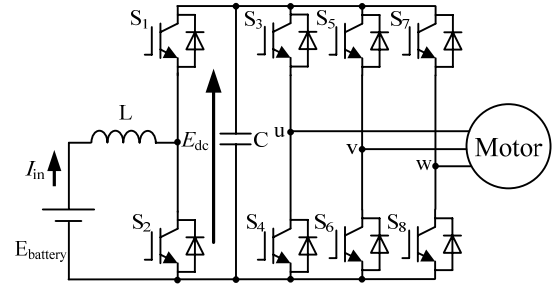
Fig. 1. Conventional circuit diagram.
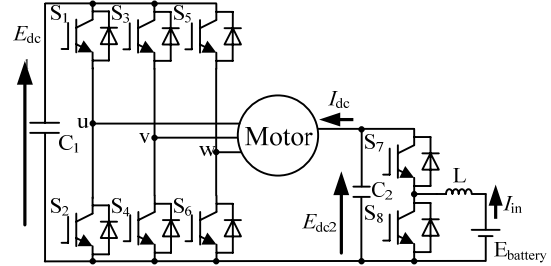
Fig. 2. Proposed circuit diagram.
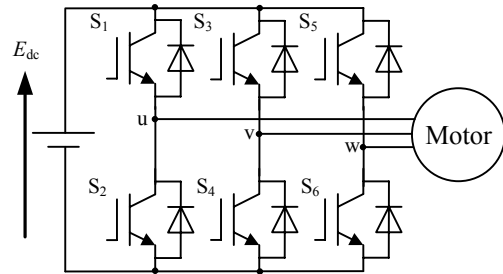
Fig. 3. Positive phase sequence equivalent circuit.
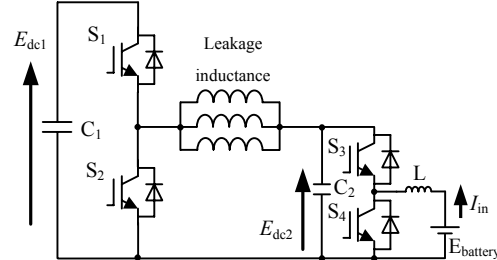
Fig. 4. Zero phase sequence equivalent circuit.

motor is given by

$$E_{dc2} = \frac{1}{3}(v_u + v_v + v_w) + \frac{1}{2} E_{dc1} \quad .... (3),$$

where E_{dc2} is the neutral point voltage of the motor, v_u, v_v and v_w are the motor phase voltage and E_{dc1} is the DC link voltage.

Therefore, the neutral point voltage of the motor can be controlled by the zero-phase voltage command. In particular, the average of the neutral point voltage of the motor for one switching period is zero when the symmetrical three-phase sinusoidal waveform is used as modulation signal. Therefore the neutral point voltage of the motor equals to double of the DC link voltage. Furthermore, sum of the maximum inverter output voltage command and the zero-phase voltage command is limited by the neutral point voltage of the motor. If the battery connects the neutral point of the motor directly, the maximum phase voltage of the motor is constrained by the battery voltage. However in the proposed circuit,

the maximum phase voltage is not constrained by the battery voltage because the neutral point voltage of the motor is controlled by the boost converter.

III. CONTROL STRATEGY

A. Control method of output voltage

Fig. 5 shows the block diagram of the proposed circuit. The control of the motor current in the proposed circuit is the same as a conventional three-phase inverter because the positive-phase sequence equivalent circuit is exactly similar to a conventional three-phase inverter. The stabilization control is applied to achieve a *V/f* control for the permanent magnetic motor [8]. The stabilization control is composed of a high-pass filter and a feed back from δ-axis current. Additionally, the PWM control is slowly changed into a six-step operation via the trapezoidal pulse modulation [9]. The transition control in Fig.5 is a proportional compensation to the amplitude of the output voltage command because the output voltage is nonlinearly increasing at the trapezoidal pulse area.

B. Battery current compensation control

In the proposed circuit, when the six-step operation is applied to the inverter control, the input current is distorting at three times of the output frequency. The reason is that the neutral point voltage of the motor has fluctuation of $\pm 1/6E_{dc1}$ with three times of the inverter output frequency in the six-step operation. In order to compensate the voltage fluctuation, a feed forward control is applied to a current regulator in the first stage boost converter. The voltage fluctuation is estimated by the DC link voltage and the pulse pattern of the inverter.

IV. SIMULATION RESULTS

A. Fundamental Operations

Table 1 shows the simulation parameters, the permanent magnet motor is 750 W, 160 V and 90 Hz, and the battery voltage is 70 V.

Fig. 6 shows the simulation results during a six-step operation. The motor model is expressed by the back EMF, the leakage inductance and the armature resistance. From Fig.6, it is confirmed that the fluctuation of the input current is suppressed by the feed forward control in the first stage boost converter. In additionally, the DC link voltage E_{dc1} is controlled to 200 V by a voltage regulator.

B. Loss analysis results

Fig. 7 shows a loss analysis comparison between the proposed circuit and the conventional circuit during a six-step operation. The loss analysis was implemented by a circuit simulator (PSIM, *Powersim Technologies Inc.*) and DLL files (Dynamic Link Library) [10]. It should be noted that in this loss analysis, the iron loss of a motor and a boost-up reactor are neglected. The loss simulation estimates that the proposed circuit can reduce the boost converter loss by 25% as compared to the conventional circuit because the proposed circuit can reduce the
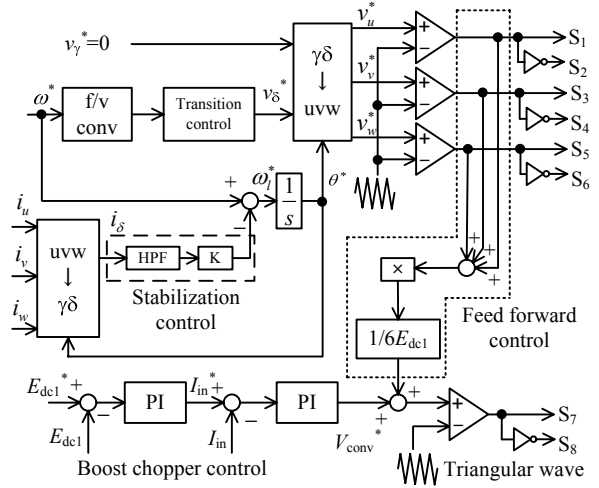
Fig. 5. Control block diagrams.

TABLE I
SIMULATION PARAMETERS

Battery volatge $V_{battery}$	48[V]
Output frequency	90[Hz]
Output power	750[W]
Rated voltage	160[V]
Rated current	3.3[A]
Boost chopper reactor L	2[mH]
Zero phase inductance	2.3[mH]
Capacitor C_1	2200[μF]
Capacitor C_2	5[μF]
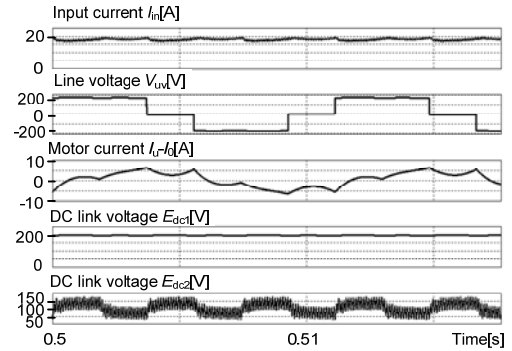
Fig. 6. Simulation results with six-step operation.
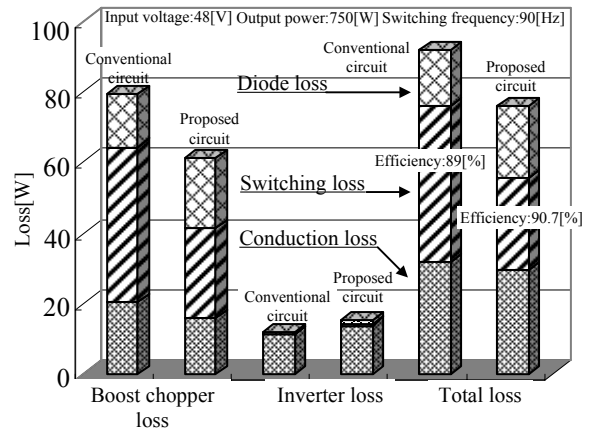
Fig. 7. Loss analysis results in simulation.

terminal voltage of a boost-up reactor. Furthermore, it also have been confirmed that the inverter switching loss is almost zero by the six-step operation. However, the inverter conduction loss is increased by the zero-phase

current. As a result, the proposed circuit improves the efficiency by 1.7% as compared to the conventional circuit.

V. EXPERIMENTAL RESULTS

A. Experimental results with PWM control

Table 2 shows the experimental parameters, the permanent magnet motor is 750 W, 175 V and 90 Hz, and the battery voltage is 70 V.

Fig. 8 shows the experimental results during a PWM control. In this experiment, the output torque is controlled to 100%. From Fig. 8, it is confirmed that the neutral point voltage of the motor is increased to double of the DC link voltage by the inverter side boost-up function that utilizes the motor leakage inductance. Furthermore, the motor current has the DC components because the motor current is added to the zero-phase current. However, the sinusoidal motor current waveform and sinusoidal line voltage of the motor are obtained. It should be noted that the output line voltage V_{uv} is observed by using a low-pass filter of 1.5-kHz cut-off frequency to observe the low frequency component distortion.

B. Experimental results with Six-step operation

Fig.9 shows the experimental result during a six-step operation. In this experiment, the output torque is controlled to 75%. In Fig. 9(a), a fluctuation occurs in the input current because the neutral point voltage of the motor has fluctuation. Fig. 9(b) shows that the ripple in the input current has been suppressed by the proposed control.

Fig. 10 shows the harmonic analysis results of the input current. In Fig. 10(a), the input current is confirmed that is containing the third harmonic components of the output frequency. For Fig. 10(b), the feed forward compensation is applied and this shows that the input current ripple has been suppressed. In comparison with Fig. 10(a), the third harmonic component of the output frequency in the input current is suppressed by 1/8 times smaller.

C. Torque Impact characteristic

Fig.11 shows the torque impact characteristic. The output frequency is 90Hz, and the step increase of torque is 100%. In Fig.11, stability to the load step can be confirmed. Furthermore, the DC link voltage E_{dc1} vibration is suppressed by a voltage regulator.

D. Acceleration characteristic

Fig.12 shows the acceleration characteristic from PWM operation to six-step operation. The PWM control is gradually changed into the six-step operation that can be confirmed by the u-v line voltage. The pulse mode moves from PWM into the six-step mode entirely without appearing of rush current.

VI. MAGNETIC FIELD AYALYSIS RESULTS

The influence about the imposed DC current is analyzed in a 2D finite element method (FEM) by

TABLE II
EXPERIMENTAL PARAMETERS

Battery volatge $V_{battery}$	70[V]
Output frequency	90[Hz]
PM motor rated output	750[W]
Rated voltage	175[V]
Rated current	3.3[A]
Boost chopper reactor L	1.7[mH]
Zero phase inductance	1.9[mH]
Capacitor C_1	1100[μF]
Capacitor C_2	5.0[μF]
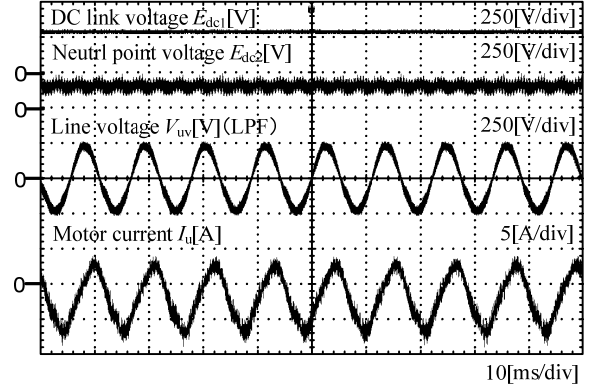
Fig. 8. Experimental results with PWM control.
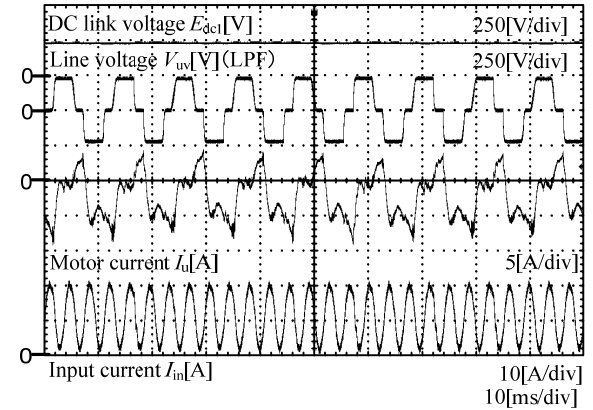
(a) Experimental results without feed forward compensation.
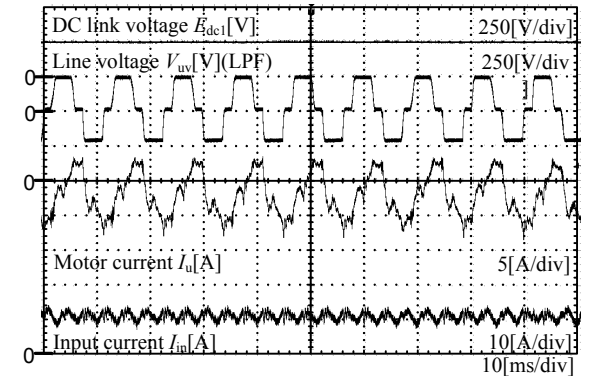
(b) Experimental results with feed forward compensation.
Fig. 9. Six-step operation experimental results.

simulating a 1.5-kW interior permanent-magnet (IPM) motor. Table 3 shows the IPM motor parameters. Two conditions are considered; first, the motor phase current is assumed as a sinusoidal rated current without the DC current. Second condition is with the DC current, where the DC current is -3.14 A per single phase.

Fig. 13 shows the magnetic flux density distribution of a 1.5-kW IPM motor. Fig. 13(a) shows the magnetic flux density distribution where the motor contains only the sinusoidal current. Fig. 13(b) shows the magnetic flux density distribution where the DC current is included. From the comparison, this shows that the magnetic flux density distribution is almost the same in both results. Therefore, this can be confirmed that the increment of the iron losses caused by the zero-phase current is very low.

Fig. 14 shows a comparison of the motor torque waveform. When the DC current is added to the output current, the torque ripple is increased by 10% because the torque ripple is affected by DC current which contains the third harmonic components of EMF and the space harmonics components. It should be noted that the torque ripple that results from the third harmonics component can be compensated by the feed forward control.

Fig. 15 shows a comparison of the IPM motor loss analysis. The copper loss is increased by the DC current component because the copper loss is proportional to the square of the motor current. On the other hand, the increase of the iron loss can be neglected. It should be noted that the motor current does not consider as carrier harmonics components by PWM.

VII. CONCLUSION

A novel two-stage DC/AC power converter connected to the neutral point of the motor has been proposed. The proposed circuit can reduce the volume of the boost-up reactor and switching losses in the boost converter. In the loss analysis, the proposed circuit improves the efficiency by 1.7% as compared to the conventional circuit. The basic operation of the proposed circuit is confirmed by the simulation and the experimental results.

A six-step operation is applied to the proposed converter with a feed forward control to compensate the fluctuation at the motor neutral point voltage. The experimental results confirmed that the proposed control method could suppress the input current distortion by 1/8 smaller.

In addition, the influence about the imposed DC current is analyzed in a 2D FEM by simulating a 1.5-kW IPM motor. The analysis shows that the torque ripple is
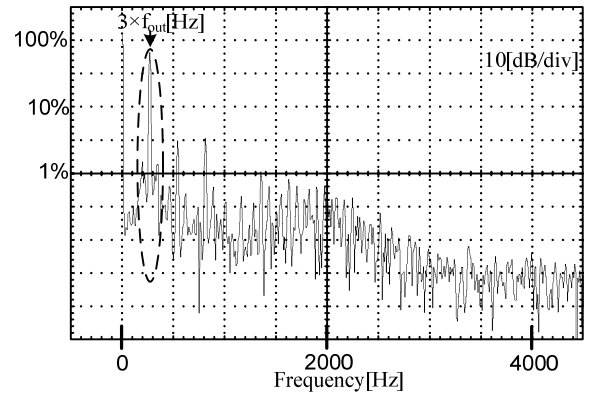
(a) Harmonics analysis without feed forward compensation.
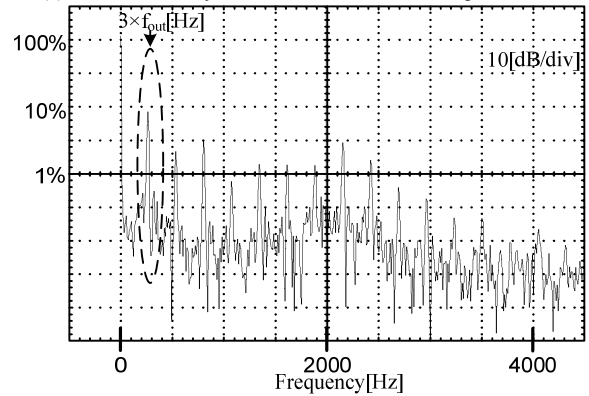
(b) Harmonics analysis with feed forward compensation.
Fig. 10. Input current harmonics analysis.
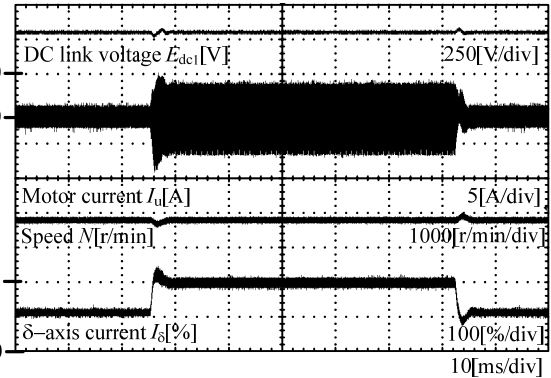
Fig. 11. Torque Impact characteristic.
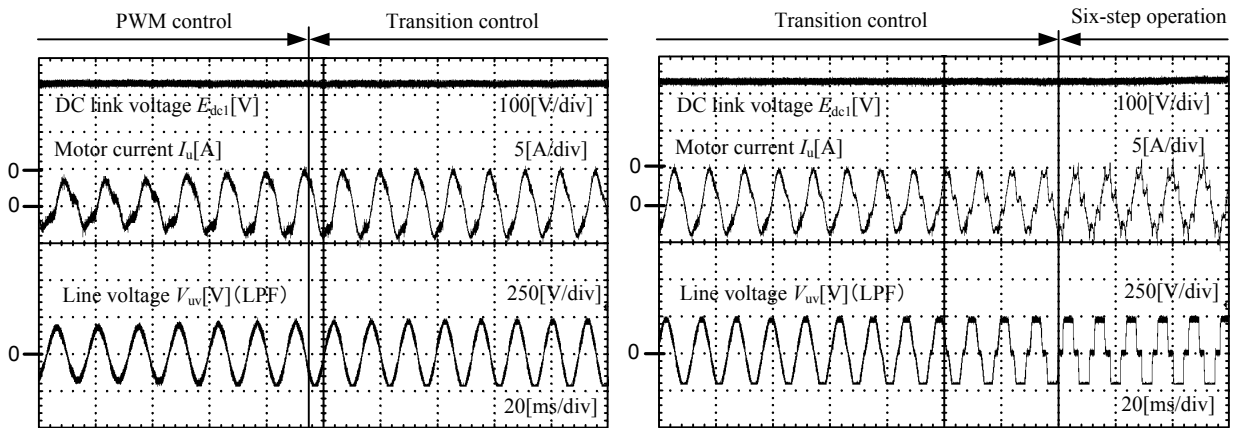
(a) Operation waveform from PWM control to Transition control.

(b) Operation waveform Transition control to six-step operation.
Fig. 12. Acceleration characteristics.

Motor Power	1.5kW
Rated Voltage	180V/phase
Rated Current	6.1A
Rated Speed	1800rpm
Number of Poles	6poles
Number of Stator Slots	36slots
Stator Outer Diameter	130mm
Stator Inner Diameter	83mm
Winding Configuration	138turn,series per phase
Rotor Outer Diameter	82.2mm
Rotor Shaft Diameter	30mm

increased by 10% and the copper loss is increased by 25%. However, the increment of the iron losses caused by the zero-phase current is very low. It should be noted that the torque ripple that results from the third harmonics component can be compensated by the feed forward control. In future work, the motor will be optimized and reduced the losses in the zero-phase current.

REFERENCES

[1] Y.Tsuruta, and A.Kawamura, "Proposal of 98.5% High Efficiency Chopper Circuit QRAS for the Electric Vehicle and the Verification," *Trans. IEEJ,* Vol.125, No.11, pp.977-987, 2005.

[2] M.Yamamoto, S.Sato, E.Hiraki, and M.Nakaoka, "New Space Vector Modulated 3-Level 3-Phase Voltage-Source Soft-Switching Inverter with Two Active Resonant DC Link Snubbers," *Trans. IEEJ,* Vol.123-D, No.12, pp.1397-1405, 2003.

[3] S.Inasaka, A.Kawamura, Y.Tsuruta "Research for High Efficient Electrical Power Management apply Bilateral Chopper for Electric Vehicle," *JIASC IEEJ*, pp.I-667-I-670, 2009.

[4] S.Nagai, S.Sato, M.Yamamoto, E.Hiraki, M.Nakaoka "Effective Improvement of DC Busline Voltage Utilization Factor in Two Switch-Auxiliary Quasi-Resonant DC Link Snubber Assisted Three Phase Voltage Source Type Soft-Switching PWM Inverter," *IEEJ Trans.* Vol.123-D, No.6, pp.710-716, 2003.

[5] J.Itoh, and S.Ishii, "A Novel Single-phase High Power Factor Converter with Load Neutral Point Applied to PM Motor Drive," *Trans. IEEJ*, Vol.121-D, No.2, pp.219-224, 2001.

[6] T. Katagiri and J.Itoh: "PM motor driving with a boost type DC/AC conversion circuit using motor neutral point," *Annual meeting of IEEJ*, pp.142-143, 2007.

[7] K.Moriya, H.Nakai, Y.Inaguma and S.Sasaki "A DC/DC Converter Using Motor Neutral Point and its Control Method," *Annual meeting of IEEJ*, Vol.4，pp.119-120, 2004.

[8] J.Itoh, J.Toyosaki, and H.Ohsawa, "High performance V/f control method for PM Motor," *Trans. IEEJ*, Vol.122-D,No.3 No.2 pp.253-259, 2002.

[9] N.Ohtani, J.Itoh "Square Wave Operation for a Single-phase PFC Three-phase Motor Drive System without a Reactor", *The International Conference on Electrical Machines and Systems*, LS4E-4, 2009.

[10] J.Itoh, and T.Iida, "Realization of High Efficiency AC Link Converter System Based on AC/AC Direct Conversion Techniques with RB-IGBT," *IEEE Industrial Electronics Conf., Paris*, pp.1703-1708, 2006.
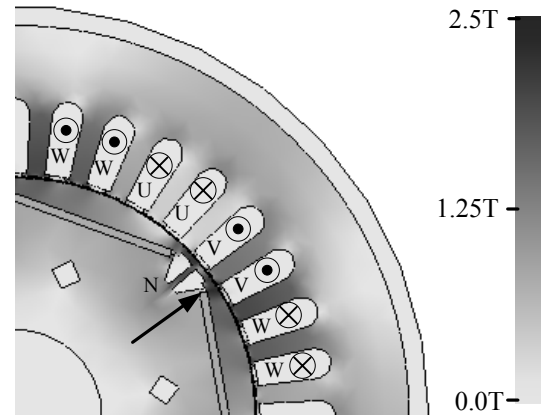
(a) Without DC current.
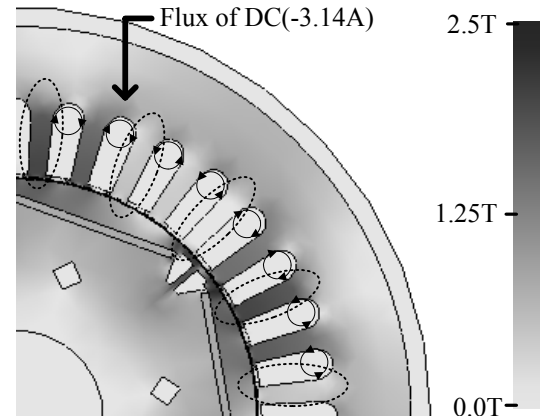
(b) With DC current.
Fig. 13. Magnetic flux density distribution.
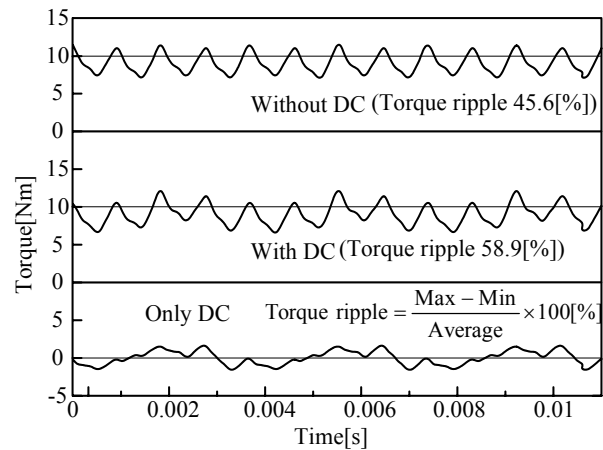
Fig. 14. Torque waveforms in simulation.
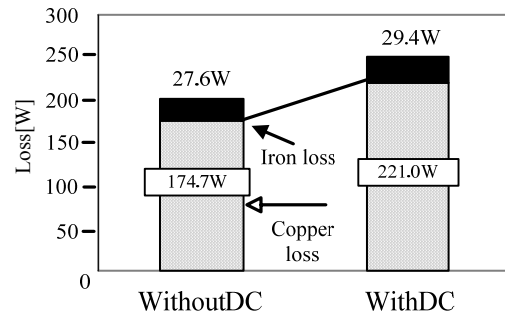
Fig. 15. IPM motor loss analysis in simulation.